JOURNAL OF GEOPHYSICAL RESEARCH, VOL. 104, NO. A3, PAGES 4609-4625, MARCH 1, 1999

Europa and Callisto: Induced or intrinsic fields in a periodically varying plasma environment

M. G. Kivelson,[1,2] K. K. Khurana,[1] D. J. Stevenson,[3] L. Bennett,[1] S. Joy,[1]
C. T. Russell,[1,2] R. J. Walker,[1] C. Zimmer,[1] and C. Polanskey [4]

Abstract. Magnetometer data from four Galileo passes by the Jovian moon Europa and three passes by Callisto are used to interpret the properties of the plasma surrounding these moons and to identify internal sources of magnetic perturbations. Near Europa the measurements are consistent with a plasma rich in pickup ions whose source is freshly ionized neutrals sputtered off of the moon's surface or atmosphere. The plasma effects vary with Europa's height above the center of Jupiter's extended plasma disk. Europa is comet-like when near the center of the current sheet. It is therefore likely that the strength of the currents coupling Europa to Jupiter's ionosphere and the brightness of a Europa footprint will depend on System III longitude. Magnetic perturbations on the scale of Europa's radius can arise from a permanent dipole moment or from an induced dipole moment driven by the time-varying part of Jupiter's magnetospheric field at Europa's orbit. Both models provide satisfactory fits. An induced dipole moment is favored because it requires no adjustable parameters. The inductive response of a conductive sphere also fits perturbations on two passes near Callisto. The implied dipole moment flips direction as is predicted for greatly differing orientations of Jupiter's magnetospheric field near Callisto in the two cases. For both moons the current carrying shells implied by induction must be located near the surface. An ionosphere cannot provide the current path, as its conductivity is too small, but a near surface ocean of ~10 km or more in thickness would explain the observations.

1. Introduction

During the primary phase of the Galileo mission, magnetic signatures were recorded by the Galileo magnetometer [*Kivelson et al.*, 1992] on close passes by the icy moons of Jupiter: Europa [*Kivelson et al.*, 1997] and Callisto [*Khurana et al.*, 1997]. Here we consider what can be learned about the interiors of these bodies and their interactions with Jupiter's magnetosphere by analyzing the magnetometer measurements. We look for evidence of magnetic perturbations generated within the moons. The presence of internally generated global-scale fields would impose significant constraints on models of the interiors of the bodies. For example, an intrinsic dipole moment either would require enough ferromagnetic material to serve as a source or would imply self-generated dynamo action that can arise if the deep interior contains conducting fluid in convective motion. Currents driven by externally imposed time-varying magnetic fields can also generate magnetic perturbations. At the Galilean moons the background field varies periodically as Jupiter's rotation changes the orientation of its tilted dipole moment. This temporally varying magnetic field can, under appropriate conditions, drive electrical currents within the moon, thereby producing perturbation magnetic fields, which we refer to as induced fields. Induced fields of surface magnitude comparable to the time-varying component of Jupiter's field require global scale conducting paths near the surfaces of the bodies. We will show that neither an icy outer crust nor a conducting global ionosphere can serve as the source of planetary scale induced magnetic fields but that for the icy moons, such induced fields can be accounted for if salty, subsurface oceans are present [*Khurana et al.*, 1998].

In an insulating environment the magnetic signatures of the internal sources would be easily identified, but the moons are embedded in the flowing plasma of Jupiter's magnetosphere. The interaction with that plasma drives localized external currents whose associated magnetic perturbations obscure the signature of an internally generated field. Those currents arise in part from the interaction of the moons with the conducting plasma that flows onto them from their trailing sides. Diversion of the plasma produces magnetic signatures that include the contributions of Alfvén wing currents [*Neubauer*, 1980; *Southwood et al.*, 1980]. In addition, the torus plasma may contain newly created ions arising from neutrals sputtered off the surface or the atmosphere of the moon. There is considerable evidence that such ions are present near Europa, both at altitudes of several Europa radii [*Gurnett et al.*, 1998] and in the vicinity of Europa's orbit [*Intriligator and Miller*, 1982]. Such ions are referred to as pickup ions, and currents appear in the plasma where they are introduced into the flow [*Goertz*, 1980]. In attempting to understand the internal field of a moon, we must identify and correct for the effects of these various external current sources. Fortunately, data from several passes by Europa and Callisto with different trajectories relative to the moons and at different locations within the Jovian current sheet help to characterize the effects of external currents and allow us to estimate separately the effects of internal and external currents. The plasma-related phenomena are found to vary in intensity with Europa's System III longitude [*Dessler*, 1983], which implies periodic variations of related phenomena such as field-aligned current magnitudes and ionospheric density profiles.

2. Magnetospheric Context of the Europa and Callisto Passes

Galileo was inserted into orbit around Jupiter on December 7, 1995. In orbit, the spacecraft acquires data of two types. For

[1]Institute of Geophysics and Planetary Physics, University of California, Los Angeles.
[2]Also at Department of Earth and Space Sciences, University of California, Los Angeles.
[3]Division of Geological and Planetary Sciences, California Institute of Technology, Pasadena.
[4]The Jet Propulsion Laboratory, Pasadena, California.

Paper number 1998JA900095.
0148-0227/99/1998JA900095$09.00

extended time intervals the field and particle instruments transmit low-rate time-averaged data in real time. Low-rate data (magnetometer samples every 24 s or more frequently) are sufficient for resolving changes on the scale of moon -radii but do not resolve details. The prime mission included three passes of Europa and three of Callisto. During passes near the moons of Jupiter and for other intervals of exceptional scientific interest, data are recorded to tape at higher rates for delayed transmission to the ground. High time resolution data are now available from two additional passes of Europa within the extended mission (Galileo Europa Mission or GEM). For the Europa and Callisto encounters, the magnetometer data rate was one vector every 0.33 s. As noted above, Jupiter's rotation combined with the 10° tilt of its dipole moment toward 202° west longitude causes the external magnetic field of Jupiter's magnetosphere and the properties of the ambient plasma in which a moon is embedded to vary periodically. A small additional variation (~15 nT near Europa's orbit) arises because of the rotation of higher-order multipole terms of Jupiter's internal field. The principal variation is periodic at the synodic period of Jupiter's rotation. In other words, external conditions at the moons vary in phase with their System III longitude. The radial component of Jupiter's magnetospheric magnetic field **B** points radially outward above the magnetic equator (here defined as the minimum |**B**| surface), points radially inward below, and passes through a node at the magnetic equator where the bulk plasma density is highest. The field components are predicted from the model of *Khurana* [1997] (hereinafter referred to as KK97). KK97 uses one of *Connerney*'s [1993] fits to Jupiter's internal field and adds the contributions of the plasma sheet currents described in terms of Euler potentials. For appropriately selected parameters of the Euler potential, KK97 provides a good fit to Jupiter's magnetospheric field along the outbound passes of Pioneer 10 and Voyager 1 and 2. For most of the Galileo passes, one or another of these models corresponds approximately to the field measured by Galileo within 30 R_J.

In Figures 1a and 1b the average radial, azimuthal, and latitudinal components of the model background magnetic field at the orbits of Europa and Callisto, respectively, are plotted versus System III longitude. Figures 1a and 1b show that the time-varying component has an amplitude of ~230 nT near Europa (synodic period of 11.1 hours) and ~40 nT at Callisto (synodic period of 10.1 hours). The locations of the moons at the times of individual Galileo passes, identified with a number, are marked in Figures 1a and 1b. The number identifies a particular orbit. Elsewhere in this paper, the passes are identified with the number of the orbit prefixed with a letter that denotes the targeted moon (E for Europa and C for Callisto). Passes well off the magnetic equator are those with the largest values of the radial component of the magnetic field, B_r. Near the magnetic equator, $B_r \sim 0$. At a fixed radial distance from Jupiter the density of the bulk plasma varies considerably with distance from the magnetic equator. *Bagenal* [1994] has characterized the variation quantitatively for the inner magnetosphere. Fortunately, the multiple encounters of both Callisto and Europa occur at different System III longitudes, thereby providing magnetic signatures in different field and plasma regimes.

During the prime mission, data were acquired exclusively in regions of relatively low magnetospheric plasma density well above the central current sheet (passes E4, E6, E11, C3, C9, and C10). (Data were not acquired by the magnetometer on pass E6.) However, the first pass (E12) in the GEM phase that followed the completion of the prime mission occurred near the center of the plasma sheet. The next pass (E14) occurred in the low plasma density region above the central current sheet. For pass E14, Galileo's trajectory relative to Europa was nearly parallel to pass E12 but with closest approach at a higher altitude and off Europa's equator.

In the ideal situation the measured magnetic field would closely track the model field until Galileo approached a moon where differences would appear. These differences would then be attributed to the moon itself. This ideal situation rarely occurs because external conditions fluctuate. In interpreting the data, we identify departures from the background field of Jupiter's magnetosphere near the moons, and we then attempt to distinguish the sources of the observed magnetic perturbations, both local and more global. Regrettably, none of the passes cross near the rotational poles of the moons, and this constrains our ability to characterize fully the internal sources.

3. External Signatures of Intrinsic and Induced Fields

The dipole moment of Earth changes significantly only over times of thousands of years. One expects similar stability for other dynamo-driven planetary magnetic fields. A planetary magnetic field produced by permanent magnetization of the crust or the core should also be stable. However, if the observed field is caused by currents induced by the time variability of the Jovian field, then it will change on a timescale of hours, and the dipole moment will be determined by the System III longitude of the observations. Thus it is, in principle, possible to separate permanent and induced internal dipole moments by comparing measurements taken at different phases of Jupiter's rotation.

In modeling an induced dipole moment, we assume that the moon is a highly conductive sphere of the size of the moon. This assumption provides the largest possible induced field. On the scale of a moon the time-varying external field of Jupiter's magnetosphere is approximately uniform spatially. In section 8 we note that the response of the conducting layer depends on the conductivity and the frequency of the driving signal. In the limit of a perfect inductive response, the induced field exactly cancels the time-varying part of Jupiter's field at the moon's surface along the radial direction from the center of the moon. (Since the response of a homogeneous sphere to a spatially uniform external field is a dipole and since the radial components of the dipolar field and external field have the same angular dependence with respect to the direction defined by the external field, this will happen everywhere on the surface.) The induction field requires interior currents large enough to exclude the radial component of the time-varying field inside of a skin depth just below the surface of the conducting layer. In the absence of plasma effects there are no adjustable parameters. In section 8 we will elaborate on the justification of such a model after having compared its predictions with the measurements.

4. Magnetometer Data From Europa Passes E4, E11, E12, and E14

Pass E4 by Europa occurred on December 19, 1996, with the closest approach at an altitude of 688 km as reported by *Kivelson et al.* [1997]. Europa orbits Jupiter in its rotational equatorial plane at a distance of 9.38 R_J (radius of Jupiter = 71,492 km). Within a range of 2 R_E from the center of the moon ($R_E \equiv$ Europa radius = 1560 km), the trajectory remained within 0.04 R_E of Europa's rotational equator. Table 1 provides additional information about this encounter and others. The trajectory was outbound from Jupiter. Near Europa the background magnetic field was tilted radially outward with a magnitude of ~450 nT.

The measured field is plotted in Figure 2a. The data are given in a Europa-centered Cartesian coordinate system, which we denote Ephio. The x axis is parallel to the direction of corotation at the time of closest approach, that is, aligned with the east longitude angle ϕ in System III. The z axis is parallel to Jupiter's spin axis, and y is radially in toward Jupiter. In Figure 3 the E4 trajectory and the trajectories of Galileo's other passes by Europa through mid-1998 are projected into the xy and yz planes of this coordinate system.

Figure 2a also shows a model of the background field of Jupiter's magnetosphere. This approximates the field that Galileo would have encountered along the portion of its trajectory through Jupiter's magnetosphere near Europa if Europa

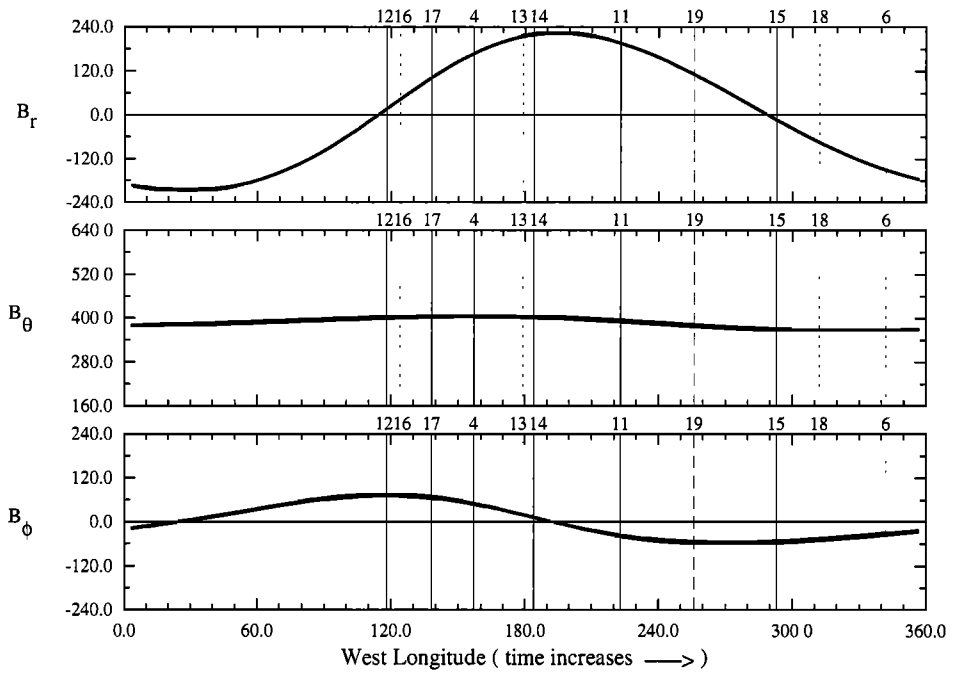

Figure 1a. Curves representing the average (top) radial, (middle) polar, and (bottom) azimuthal components (B_r, B_θ, B_ϕ) of the magnetic field at the position of Europa as a function of its west longitude relative to the origin of System III. (Note that for System III, west longitude is standard, but the field vectors are represented in a right-hand coordinate system. Thus B_ϕ is positive in the sense of corotation.) The field model used is that developed by *Khurana* [1997] for the conditions of the Pioneer 10 pass. Orbits on which passes by Europa occur are labeled by number at the top of the plots with vertical markers showing where the passes occur relative to west longitude. Dotted lines are used for passes on which no magnetometer data are available. Dashed lines are used for passes that have not yet occurred. (There are or should be high time resolution magnetometer data for passes E4, E11, E12, E14, E15, E16, and E19 and low time resolution data for passes E17 and E18.) The magnitude of the radial component of the field increases monotonically with distance from the center of the plasma sheet while the plasma density decreases. Passes at large B_r occur near the north-south boundaries of the plasma sheet and correspond to local minima of torus plasma density. Note that passes E4 and E11, discussed in section 4, both occurred in regions of relatively low density.

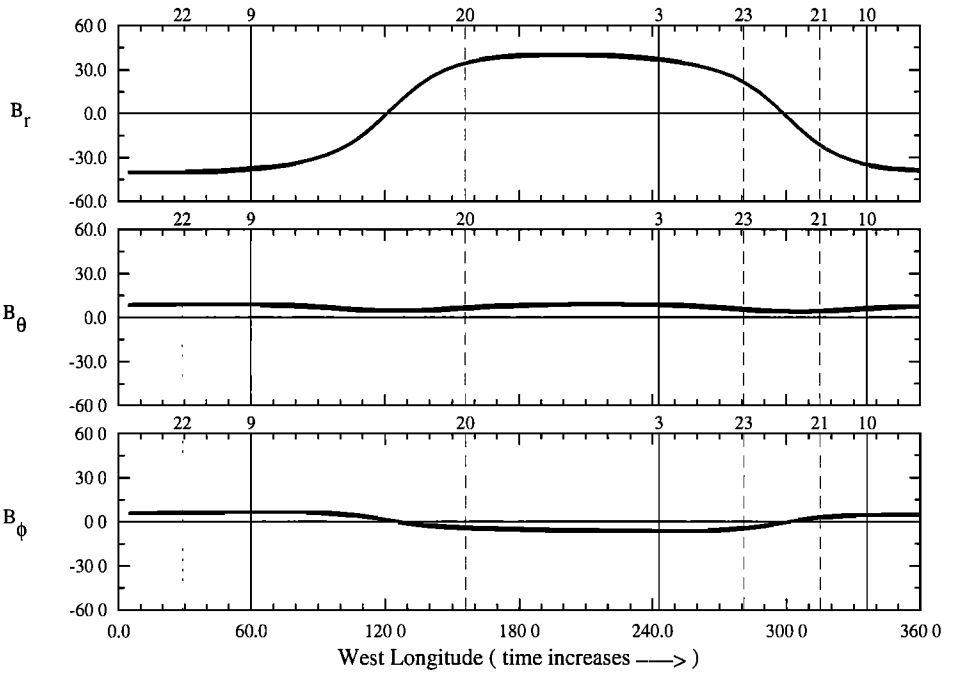

Figure 1b. The equivalent of that presented for Europa in Figure 1a but for Callisto. Note that passes C3, C9, and C10, discussed in section 5, all occurred in regions of low relative density. (There are high time resolution data for passes C3, C9, and C10. There will be low time resolution data for passes C20, C21, and C23.)

Table 1. Europa and Callisto Passes

Pass	Date	Time,[a] UT	Altitude, km	Latitude,[b] deg	West Longitude,[c] deg	System III Latitude, deg	System III West Longitude, deg	Magnetic. Latitude,[d] deg	Local time
				Encounters Through March 1998					
E4	Dec. 19, 1996	0652:58	688	–1.6	38	–0.2	157	6.6	1642
E11	Nov. 6, 1997	2031:44	2039	25.7	141	–0.3	223	8.7	1057
E12	Dec. 16, 1997	1203:20	196	-8.6	226	–0.1	118	0.9	1439
E14	Mar. 29, 1998	1321:16	1641	12.0	229	0.0	184	9.1	1425
C3	Nov. 4, 1996	1334:28	1139	13.2	78	–0.2	243	7.1	0748
C9	June 25, 1997	1347:50	421	2.0	259	–0.2	60	-7.8	0532
C10	Sept. 17, 1997	0018:55	538	4.6	79	–0.2	336	-6.9	0502
				Anticipated Additional Encounters in GEM					
E15	May 31, 1998	2112:23	2515	14.9	135	–0.3	293	-0.5	1004
E16	Jul. 21, 1998	0504:43	1830	–25.6	226	–0.1	124	1.9	1348
E17[e]	Sept. 26, 1998	0351:03	3588	–42.5	140	–0.6	138	3.6	0954
E18[e]	Nov. 22, 1998	1144:56	2276	41.7	221	0.2	312	-3.1	1304
E19	Feb. 1, 1999	0211:35	1480	31.0	331	–0.1	256	5.6	0948
C20[e]	May 5, 1999	1400:51	1316	2.5	102	0.2	156	6.9	1750
C21[e]	June 30, 1999	0745:34	1051	–0.8	74	–0.2	315	-4.0	0145
C22[f]	Aug. 14, 1999	0834:01	2293	–3.2	108	0.1	29	-9.4	1809
C23[e]	Sept. 16, 1999	1730:05	1058	–0.5	110	0.1	281	1.9	1754

[a]Time of closest approach (universal time at the spacecraft).
[b]Latitude in degrees relative to the moon's equator.
[c]West longitude at closest approach. By convention, the origin of longitude is at the Jupiter-facing meridian plane.
[d]Magnetic latitude relative to Jupiter's magnetic equator.
[e]No recorded data on this pass. Only real time data will be acquired.
[f]Neither recorded nor real time data on this pass. The Galileo magnetometer will acquire 30 s averages during the flyby.

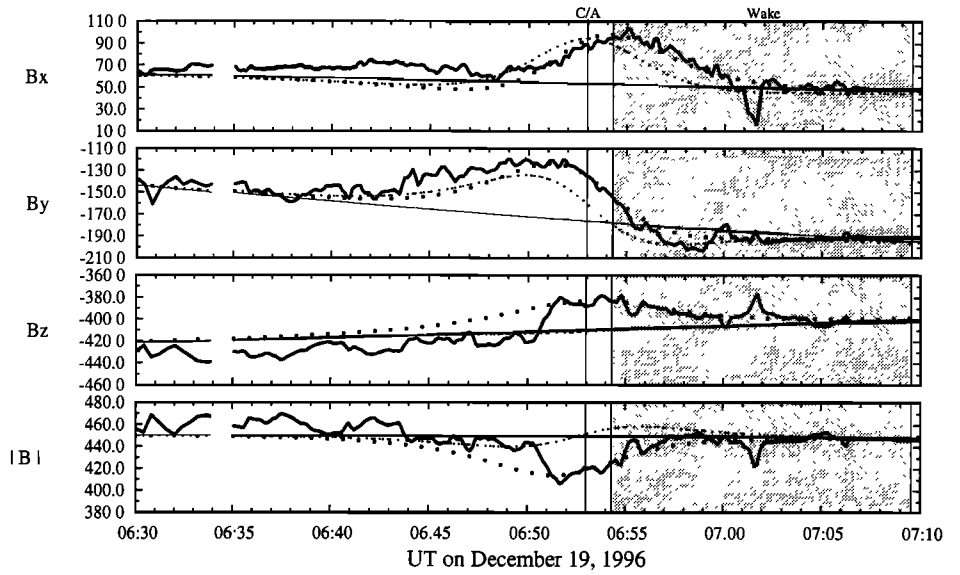

X	-2.36	-1.48	-0 57	0.31	1 22	2.08	2 94	3.77
Y	3 33	2.75	2.15	1 55	0.90	0.25	-0.42	-1 07
Z	-0.05	-0.05	-0.04	-0.04	-0.03	-0 02	-0.01	-0.01
R	4 09	3 13	2.23	1 58	1 52	2.09	2 97	3.92

Figure 2a. Ten second average plot of the measured components and magnitude of the magnetic field for Europa pass E4 of December 19, 1996 (thick solid curves). The coordinate system (Ephio) is Europa-centered with x along the direction of corotation, y radially inward toward Jupiter, and z parallel to Jupiter's rotation axis. The location of the closest approach is marked. Also, intervals within the geometric wake relative to the corotating plasma are shaded. Distances along the trajectory (in units of Europa-radii, R_E = 1560 km) are labeled at the bottom. The thin solid curves show the background magnetic field evaluated as described in the text. The dashed curves show the sum of this background field and the field of an induced dipole. The traces drawn by solid circles show the sum of this background field and the field of a best fit dipole evaluated to fit this pass. The best fit internal dipole was determined using data obtained from the period 0640- 0705 UT.

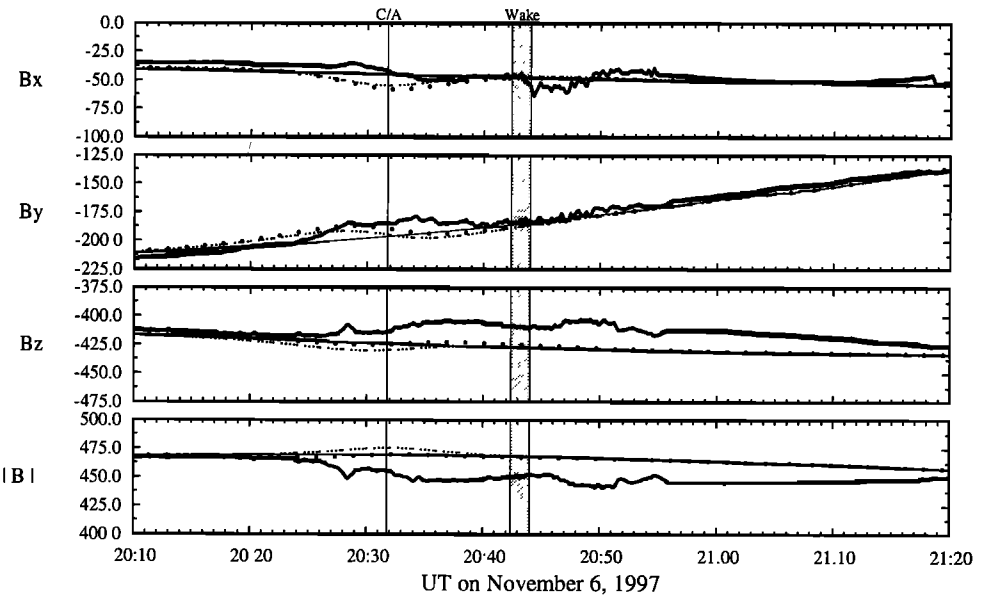

X	-2.43	-0.71	1 01	2.71	4.38	6.04	7.68	9.33
Y	-4.57	-3.23	-1.86	-0 45	0.97	2.38	3 79	5.20
Z	0.92	0.96	0.99	0.99	0.99	0.98	0.97	0.96
R	5 26	3 44	2.33	2.92	4.59	6.56	8.62	10.72

Figure 2b. Same as Figure 2a but for pass E11 of November 6, 1997.

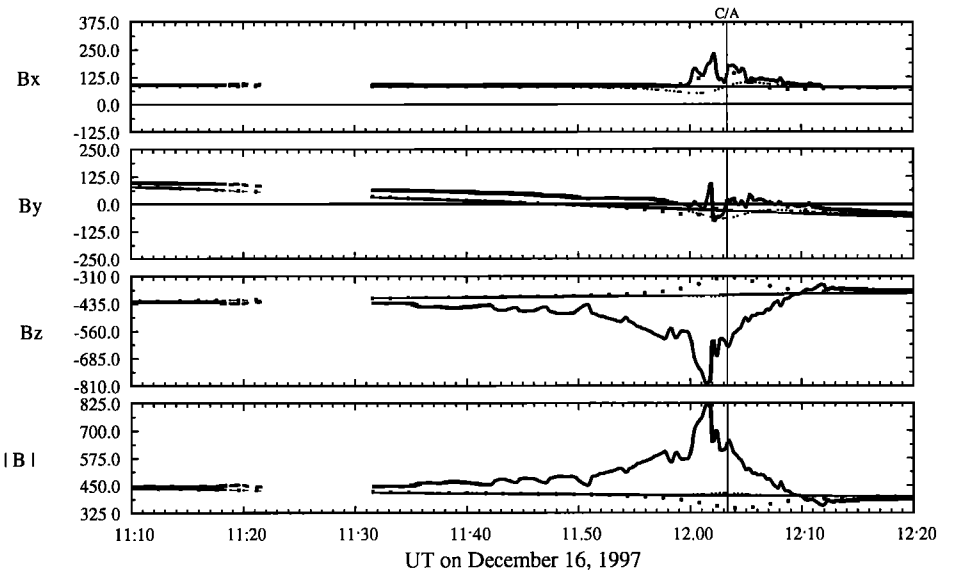

X	-9 15	-7.60	-5.81	-4.50	-2.94	-1 34	0.36	2.08
Y	8 44	6.72	4.72	3.27	1.54	-0.20	-1.89	-3.49
Z	-0.08	-0 10	-0 12	-0.14	-0 16	-0.17	-0.17	-0.16
R	12 45	10.15	7.48	5.57	3.32	1.37	1.93	4.06

Figure 2c. Same as Figure 2a but for pass E12 of December 16, 1997. The data have been recovered from partial saturation for the interval between 1153:01 and 1205:16 UT. In this interval, the measurement uncertainties are a few percent.

had not been present. It has been estimated by fitting a third-order polynomial to roughly 3 hours of the low time resolution magnetic field measurements surrounding closest approach (CA), after excising measurements taken within 5 R_E of Europa.

Figure 2a also shows the field along the trajectory from two different models. The dipole (FD-E4) model [*Kivelson et al.*, 1997] was found by fitting a Europa-centered dipole to the difference between the background field described above and the measurements. The dipole has a surface field of 120 nT at the equator (240 nT at the magnetic pole). It is tilted at 135° relative to the spin axis and rotated 20° west of the Jupiter facing meridian. This three-parameter model gives a reasonable approximation to the trend of changes with scale lengths of a few Europa radii corresponding to temporal variations with periods of

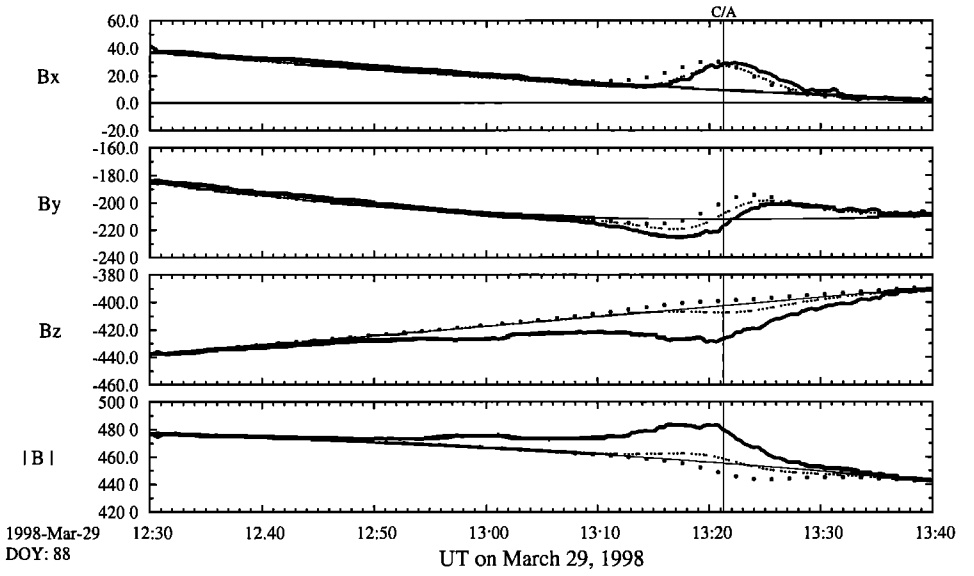

X	-9.84	-8.17	-6.56	-4 95	-3.31	-1 65	0.05	1.75
Y	8.06	6 16	4.34	2.51	0.67	-1 16	-2.96	-4.72
Z	0.29	0 32	0.34	0.37	0.40	0.42	0.43	0.43
R	12.72	10 24	7.87	5.56	3.39	2.06	2.99	5.06

Figure 2d. Same as Figure 2a but for pass E14 of March 29, 1998.

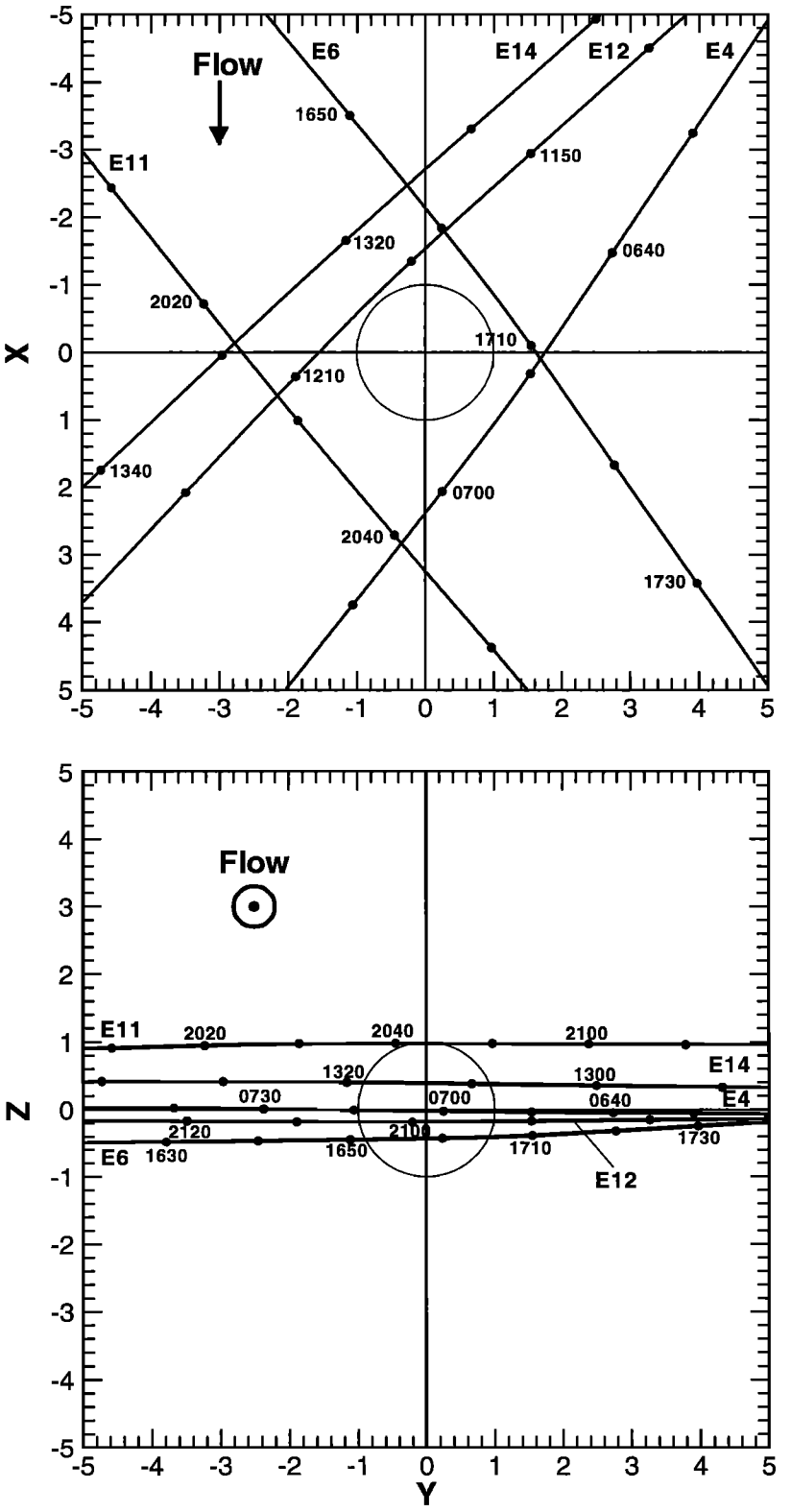

Figure 3. Trajectories of Galileo's passes E4, E11, E12, and E14 past Europa projected into the *xy* and *yz* planes of the Ephio coordinate system defined for Figure 2.

~15 min. Numerous short-timescale signatures such as the large increase in B_z observed at 0650-0651 UT must relate to plasma processes, as we discuss below, and are not reproduced by the FD-E4 model.

As for any dipole fit, one can resolve the FD-E4 model into two components: a spin axis aligned dipole moment $\mathbf{M}_z$, here oriented southward, and a transverse dipole in the *xy* plane, $\mathbf{M}_\perp$. Each of these dipole moments has a surface equatorial field magnitude of ~85 nT. As the E4 trajectory is very close to Europa's equator, it is the measured value of B_z that determines $\mathbf{M}_z$, while $\mathbf{M}_\perp$ is determined by the other two components, $\mathbf{B}_\perp$. The FD-E4 model probably represents $\mathbf{M}_\perp$ more accurately than

it represents $\mathbf{M}_z$. This is because near the moon's equator, $\mathbf{M}_z$ produces a field oriented mainly along the z direction. However, B_z may be strongly modified by plasma-related signatures. In particular, the anticipated field-aligned currents flowing in the plasma converge in the equatorial plane where they close across the field. Thus they generate perturbations in the z direction with negligible transverse components. Plasma pickup currents and diamagnetic currents generated by newly pickedup warm plasma also mainly change the field strength, hence B_z. On the other hand, the transverse components of the field near the equatorial plane arise principally from $\mathbf{M}_\perp$ and not from plasma effects. Practically, if $\mathbf{M}_\perp$ is better known than $\mathbf{M}_z$, the tilt of the dipole is less well determined than its meridian and its magnitude.

Because the strength of plasma currents also varies at the synodic period of Jupiter, plasma-related magnetic fields may induce currents in the conducting interior. However, from the argument above it is apparent that near the equatorial plane of Europa the plasma-related fields and the induction field caused by the plasma-related fields would both affect mainly the B_z component. This uncertainty also affects principally the determination of $\mathbf{M}_z$.

The additional model field plotted in Figure 2a is the response anticipated if the perturbations arise from a perfect inductive response of a conducting sphere of radius 1 R_E. In such a case, induced currents produce a dipole whose polar field at the surface of the sphere precisely cancels the instantaneous time-varying component of the background field. At the time of closest approach the background field was B_x = 53 nT, B_y = −176 nT. Here we have ignored the small periodic variation of B_z. This means that the induced dipole (ID), $\mathbf{M}_\perp$ (tilted at 90° relative to the spin axis), is rotated 17° east of the Jupiter facing meridian, with an equatorial field strength of 92 nT. The induced dipole model gives contributions to B_x and B_y that are shifted in phase relative to the FD-E4 model, but they generally follow the form of the transverse perturbations.

The fluctuations of ~10 to 20-nT amplitude and characteristic periods shorter than 15 min that appear in Figure 2a over a distance of several R_E from Europa must arise from currents in the plasma. Near Europa's orbit, the fluctuation amplitudes in the background plasma rarely exceed several nanotesla. (This can be confirmed by reference to data obtained at distances greater than 7 R_E from Europa in Figures 2b-2d.) The fluctuations seen in Figure 2a are common in regions where the plasma contains newly ionized matter. A source for such new ions is neutral particles sputtered from Europa and its atmosphere [*Eviatar et al.*, 1981, 1985; *Cheng et al.*, 1986; *Schreier et al.*, 1993; *Ip*, 1996; *Ip et al.*, 1998; *Saur et al.*, 1998]. As in a cometary environment, the plasma flowing upstream of the moon can be slowed by direct interaction with a conducting moon or by pickup ions introduced into the flow; such slowing probably accounts for the positive perturbation in $|\mathbf{B}|$ where $x < 0$ before ~0648 UT. Downstream of the moon (i.e., where $x > 0$) the flow accelerates, thus accounting for the negative perturbation in $|\mathbf{B}|$ after that time.

Another plasma-related signature in Figure 2a is the field depression just before 0702 UT. It occurs within 0.1 R_E of the middle of the geometric wake of Europa, downstream in the corotating flow of Jupiter's magnetospheric plasma, and it is indubitably the signature of compressed plasma (an interpretation consistent with plasma data from *Paterson et al.* [1998]).

From pass E4 alone there is no way to determine whether the modeled dipole moment relates to an internal field of Europa. However, the good correspondence between the measured transverse field perturbations and the predictions of both the FD-E4 model and the ID model suggests that internal currents contribute to the interaction. It is interesting, therefore, to analyze the data from other passes with these models in mind.

Figure 2b shows data from pass E11 by Europa. The data were acquired on November 6, 1997, on a pass inbound toward Jupiter. Closest approach occurred at the rather high altitude of 2039 km = 1.31 R_E. Again, the external field was tilted outward from Jupiter with B_x = −45 nT, B_y = −196 nT, but on this pass the field was decreasing in magnitude. Figure 2b also shows the total field predicted by adding either the FD-E4 fit from pass E4 or the ID field to the background field. For encounters above the current sheet including E11, E14, and E4, the induced dipole moment points close to the Jupiter facing meridian as does $\mathbf{M}_\perp$ of FD-E4, implying that near Europa's equator there will be little to distinguish the two models. On pass E11, the induced dipole moment has an equatorial field strength of 101 nT. It is rotated 13° west of the Jupiter facing meridian, that is, it lies in the same meridian plane as the FD-E4 dipole moment. Unfortunately, because the altitude of closest approach was rather large for this encounter, the predicted amplitudes are small, of the same order as perturbations produced by plasma currents. The trajectory brings Galileo close to Europa only downstream in the flow ($x >$ 0 after 2024 UT) where the field magnitude drops sharply in the region where the plasma is expected to reaccelerate. The matches are poor for both the FD-E4 model and the ID model. Plasma effects appear to dominate the signature of internal currents. Thus, although the data do not confirm either a permanent internal field or an induced field, they do not necessarily exclude such sources.

Figure 2c shows data from pass E12 by Europa outbound from Jupiter on December 16, 1997, with closest approach at 1203 UT at an altitude of 196 km. The KK97 model places the central current sheet crossing at 1154 UT. Thus this encounter occurred upstream in the plasma flow at the center of the plasma torus, i.e., in the region where Europa encounters the highest plasma density. When recorded data began following a 10-min data gap, the field was already noticeably enhanced above the background field at a range of more than 7 R_E. The amplitude continued to grow, reaching nearly double the background value shortly before closest approach, and after closest approach it dropped back to model values at a range of roughly 2 R_E. Again, on this pass, the decrease below the background field occurred close to the time when the trajectory crossed $x = 0$ at 1207 UT.

The models of perturbations produced by currents internal to Europa are plotted in Figure 2c. For this pass with B_x = 78 nT, B_y = −31 nT in the background field, the ID is rotated 68° east of the Jupiter facing meridian with an equatorial field strength of 42 nT. The ID model predicts only small perturbations (maximum near 35 nT) because the time-varying component of the field is negligibly small as is evident in Figure 1. Compared with the measured transverse perturbations, they are too small to be detected.

The FD-E4 model predicts significant but not dominant perturbations (as large as ~115 nT), and it models reasonably well the general trend of the components perpendicular to the spin axis. The predicted z perturbation is small and opposite in sign to the observed perturbation. The poor agreement of the z component of the perturbation was a feature of the other passes as well and results from field compression related to phenomena such as plasma slowing and reacceleration.

Figure 2d presents analogous data and models for the E14 pass. The data were acquired on March 29, 1998, on a trajectory similar to E12 but at higher altitude and latitude relative to Europa (see Figure 3). Closest approach occurred at an altitude of 1641 km = 1.05 R_E. Again, the external field was tilted outward from Jupiter (Figure 1a). The FD-E4 and ID model traces are also plotted. For this pass with B_x = 9 nT, B_y = −212 nT in the background field, the induced dipole is rotated ~2° east of the Jupiter facing meridian with an equatorial field strength of 106 nT. Both the FD-E4 and the ID models fit the transverse components of the data rather closely, and again, for this pass the differences in the predictions from the two models are small. We will return to a discussion of the signatures and provide further interpretation after introducing the data from the first three passes by Callisto.

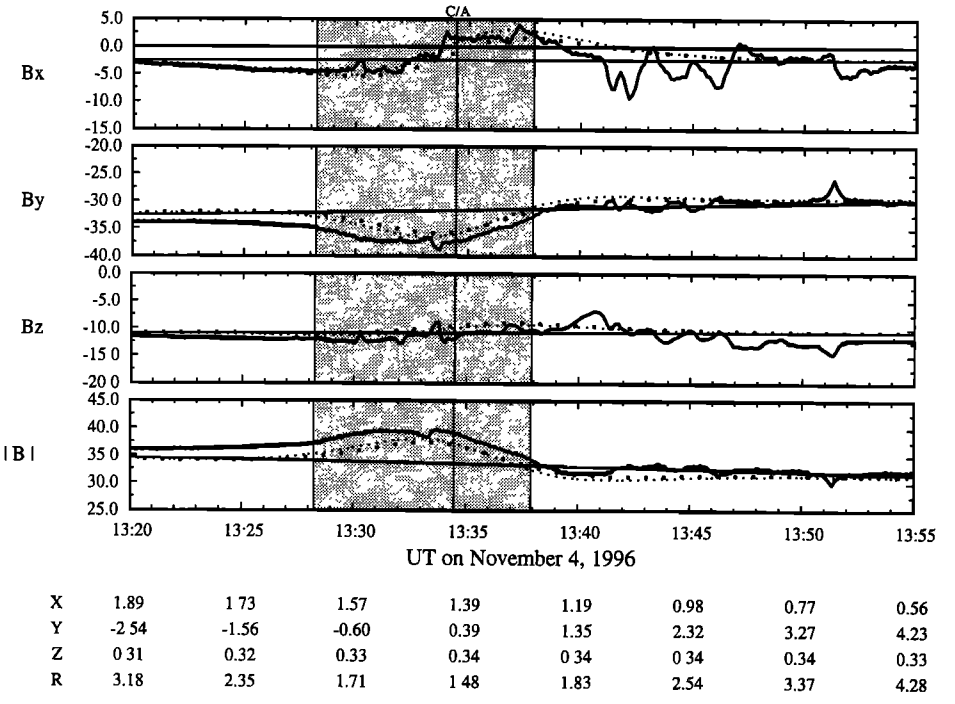

X	1.89	1 73	1.57	1.39	1.19	0.98	0.77	0.56
Y	-2 54	-1.56	-0.60	0.39	1.35	2.32	3.27	4.23
Z	0 31	0.32	0.33	0.34	0 34	0 34	0.34	0.33
R	3.18	2.35	1.71	1 48	1.83	2.54	3.37	4.28

Figure 4a. Ten second averages of the measured components and magnitude of the magnetic field as in Figure 2 but for Callisto pass C3 of November 4, 1996. The coordinate frame is analogous to that defined for Europa but is Callisto centered (hence Cphio) and in units of Callisto radii (R_C = 2409 km). Data are plotted with thick solid curves. Line styles are as defined for Figure 2a. The best fit internal dipole was determined by using magnetic data from the period 1320-1350 UT.

5. Magnetometer Data From Callisto Passes C3, C9, and C10

The first pass by Callisto (C3) occurred on November 4, 1996, with closest approach at an altitude of 1139 km as reported by *Khurana et al.* [1997]. Callisto orbits Jupiter close to its rotational equatorial plane at a distance of 26.33 R_J. Khurana et al. concluded that any internal field must be very small, and they provided an upper limit to an internal field by fitting a dipole moment to the difference between the measured field and the model background field. This fitted Callisto-centered dipole (FD-C3) has a surface field of ~14 nT at its magnetic equator, is tilted at 80° relative to the spin axis, and points approximately toward Jupiter. Figure 4a shows the magnetic field measurements for pass C3. Figure 4a also shows the polynomial fit to the background field and the background field summed both with the FD-C3 and with an ID field model whose dipole moment points 4° west of the Jupiter facing meridian with an equatorial surface field of 16 nT. The latter two traces differ little. Both represent the Callisto-scale variations quite well, as is noted by *Neubauer* [1998a]. The absence of fluctuations on scales that are small compared with the radius of Callisto in the first 10 min of the pass suggests that plasma effects may be relatively minor, although they grow and become large after ~1340 UT.

In Figure 4b we show the data from pass C9 in the same format as that for the other passes. This pass occurred on June 25, 1997, at an altitude of 421 km. The perturbations predicted by the FD-C3 model are roughly of the magnitude of the observed perturbations but of opposite sign, indicating that this model is unsatisfactory. On the other hand, an ID model that has a dipole moment pointing 177° west of the Jupiter facing meridian and that has an equatorial surface field of 17 nT approximates the dominant perturbations quite closely. Plasma fluctuations are small.

Figure 4c presents the analogous data and models for pass C10 of September 17, 1997, with closest approach at an altitude of 538 km. The FD-C3 model is also plotted here. The ID model whose dipole moment points 172° west of the Jupiter facing meridian with an equatorial surface field of 15 nT is shown. For this pass, the short-wavelength fluctuations are as large as or possibly larger than the changes on the scale of Callisto's radius, and contributions from internal sources are obscured. Projections of pass C3 and Galileo's other trajectories by Callisto through mid-1998 are plotted in Figure 5.

6. Inferences Regarding Properties of the Ambient Plasma

From the data for four Europa passes, it is dramatically evident that plasma conditions dominate the variability of the signatures. Fluctuations or systematic departures from the background field begin so far upstream of Europa (~4 R_E for pass E4, ~8 R_E for pass E14, and ~10 R_E for pass E12) that intrinsic field perturbations cannot be responsible. However, a cloud of neutrals sputtered from Europa could produce effects over a very extended region. It is known that the plasma in the region surrounding Europa appears rich in newly injected ions and electrons. *Gurnett et al.* [1998] has reported that the plasma wave (PWS) [*Gurnett et al.*, 1992] spectra reveal a region of highly disturbed plasma with density enhancements of roughly a factor of 2 above ambient densities surrounding Europa in a volume of several Europa radii on both pass E4 and pass E6. They detected enhanced whistler wave noise in the vicinity of Europa. Whistler waves grow readily when the charged particle distributions are anisotropic in velocity space, and they may develop in regions of pickup ions.

Plasma newly introduced near Europa produces the most dramatic signature in the data for E12 where the background

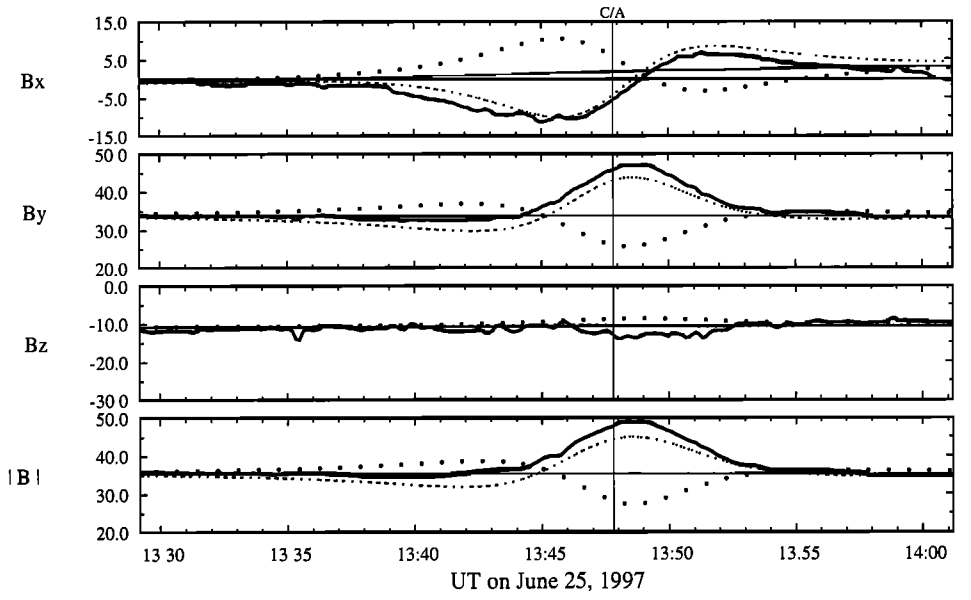

X	-0.45	-0.66	-0 86	-1.06	-1.23	-1.38	-1.51
Y	-3.74	-2.74	-1.77	-0 76	0.24	1.26	2 25
Z	0.01	0.02	0.03	0 04	0 05	0.05	0.06
R	3.76	2.82	1.96	1 30	1 25	1.87	2 71

Figure 4b. Same as Figure 4a but for pass C9 of June 25, 1997. The best fit internal dipole was determined from the data obtained from pass C3.

electron number density was significantly enhanced relative to the other passes (D. A. Gurnett and A. Roux, personal communication, 1998). The magnetic perturbations differ in character inside and outside of ~1.4 R_E from the center of Europa. Outside of 1.4 R_E, the perturbations are field-aligned, changing gradually in amplitude. The field is significantly compressed upstream of Europa and slightly depressed downstream. We attribute the compression to the slowing that occurs as momentum is extracted from flow and fed into the thermal motion of newly added ions or carried off by the neutral products of charge exchange [*Linker et al.*, 1991]. If flow divergence is small, as the flow slows, the magnetic field magnitude increases in order to conserve magnetic flux. In this case, the perturbation field increase from a background value of

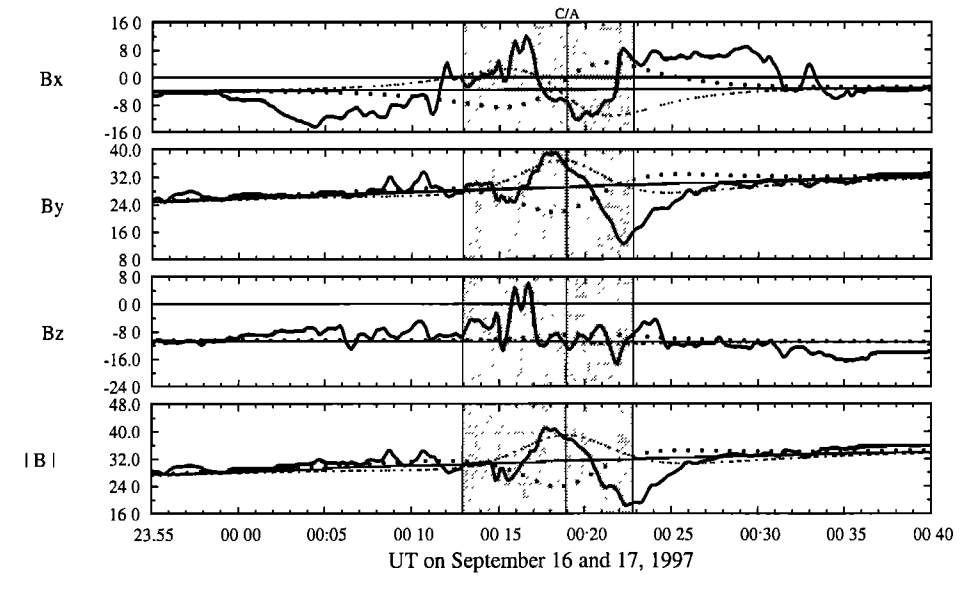

X	1.90	1 77	1.63	1 48	1.33	1.16	0 96	0 76	0 55	0.34
Y	-4 56	-3.58	-2 57	-1.58	-0.57	0 43	1 45	2.43	3 43	4.39
Z	0 06	0 07	0.08	0 09	0.09	0.10	0.10	0.10	0.10	0.11
R	4 94	3 99	3 04	2 17	1.45	1.24	1 74	2.55	3.47	4.41

Figure 4c. Same as Figure 4a but for pass C10 of September 16, 1997. The best fit internal dipole was determined from the data obtained from pass C3

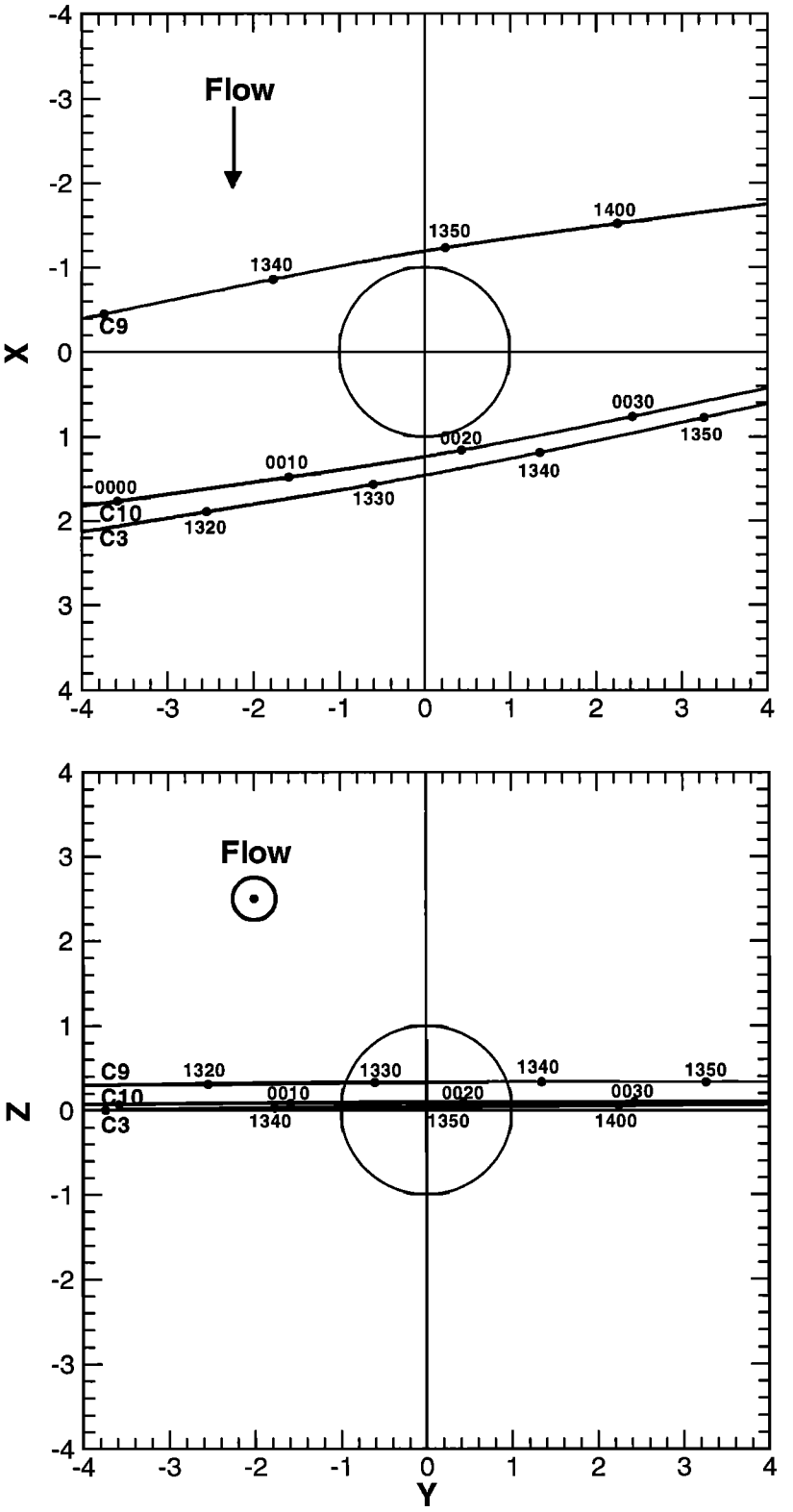

Figure 5. Same as Figure 3 but for passes C3, C9, and C10 past Callisto in the Cphio coordinate system.

410 - 440 nT to ~600 nT at a range of 1.36 R_E would imply that the flow speed has decreased by a factor of 0.7. Correspondingly, the density changes by an amount that depends on the source rate and the pickup mechanism. If impact ionization dominates, the density must increase, but if charge exchange dominates, the density may not change significantly. The signature of a density increase was not observed on the PWS spectra (A. Roux, personal communication, 1998). This could imply that charge exchange dominates, but it should be noted that as Galileo approached Europa, it was outbound and moving away from the center of the plasma sheet. It is quite plausible that the electron number density remained close to constant despite the addition of newly formed ion-electron pairs until the spacecraft began to move away from Europa. Fluctuations evident in the

compressional component are probably related to the nonlinearity of the pickup process. The speeding up of the flow downstream of Europa can account for the field depression that appeared in the $x > 0$ portion of the trajectory.

Inside of 1.4 R_E on E12 the field magnitude increases at a rapid rate to a peak almost double that of the ambient field shortly upstream of closest approach. At 1202 UT the transverse perturbations become large, with fluctuations suggestive of strong field-aligned currents (see Figure 2c). It seems likely that in this inner region, additional processes related to diversion of the flow and Alfvén wing interactions supplement pickup, bending the field and further increasing its magnitude. The peak occurs between the center of Europa's cross section relative to the flow direction ($x = 0$) and closest approach, which is where one would expect to encounter the slowest flow along the Galileo orbit in a plasma that is approaching an obstacle.

The relative amplitudes of the perturbations on the four passes differed dramatically as is shown in Figure 6. Part of the difference relates to differing distances of closest approach and the symmetry of the passes relative to the flow. Even allowing for such trajectory-related differences, we think it is significant that the size and scale of the perturbation were largest on the only pass (E12) that encountered Europa within the high-density regions near the center of the plasma torus. Although the low altitude of closest approach was unique to the E12 encounter (see Table 1), the magnitude of the perturbation signature would have been notable on this pass even if the approach had been no closer than that on E4. Indeed, on E12 at the altitude (~700 km) of the E4 closest approach, the perturbations were 160 nT inbound and 80 nT outbound whereas the largest perturbation in |**B**| observed on E4 was 36 nT.

Support for an interpretation relating the magnitude of the signature at E12 to its location in the plasma sheet is found by comparing E12 with E14. On E12, not only was the maximum perturbation almost an order of magnitude larger than that on the other passes, but even at the altitude (~1641 km) of the E14 closest approach, the E12 perturbation (~150 nT) was almost 5 times larger than the largest perturbation in |**B**| observed on E14. Both the E14 trajectory and the E12 trajectory started upstream of Europa and ended downstream. Both came closest to the surface on the outward facing upstream side. The passes occurred at similar local times (see Table 1). Thus the large differences between the field perturbations detected on the two passes (maximum perturbation of ~400 nT on E12 and maximum perturbation of <50 nT on E14) must relate to the location of these two passes within the plasma torus. E12, at System III west longitude of 118°, encountered Europa approximately when it was embedded in the highest plasma density along its orbit. E14, at System III west longitude of 184°, encountered Europa approximately when it was embedded in the lowest plasma density along its orbit. We believe that the great differences in the signatures arise because of this difference in the plasma environment.

Our results imply that the rate of plasma pickup varies periodically, and by inference, the neutral cloud density surrounding Europa is significantly modulated by its System III longitude. Europa appears most like a comet when near the center of the plasma sheet. Its response to its periodically changing environment is consistent with the time-varying properties of the plasma that sputters the neutrals into Europa's environment. Where pickup is most important, the interaction with the torus plasma would possibly enhance ionospheric densities, and it is likely to generate the most intense field-aligned currents coupling Europa to Jupiter's ionosphere. This suggests that a footprint signature of Europa in Jupiter's ionosphere is most probable for footprints at System III west longitudes near 117° and 286°, where Europa crosses the current sheet (see $B_r = 0$ in Figure 1a).

At Callisto the perturbations do not vary systematically with distance from the moon. Rather they are fluctuations that could be intrinsic to the plasma torus or related to external disturbances. There are no features that we find suggestive of extensive clouds of pickup ions around the moon. However, none of the passes has occurred near the magnetic equator, and it will be interesting to seek evidence of the effects of System III modulation of the plasma environment at Callisto in the data of subsequent passes.

7. Inferences Regarding Internal Sources of Magnetic Perturbations

The features described in section 6 above that we associate with plasma effects are either too extended in space or of short duration and therefore too localized in space to be the signatures

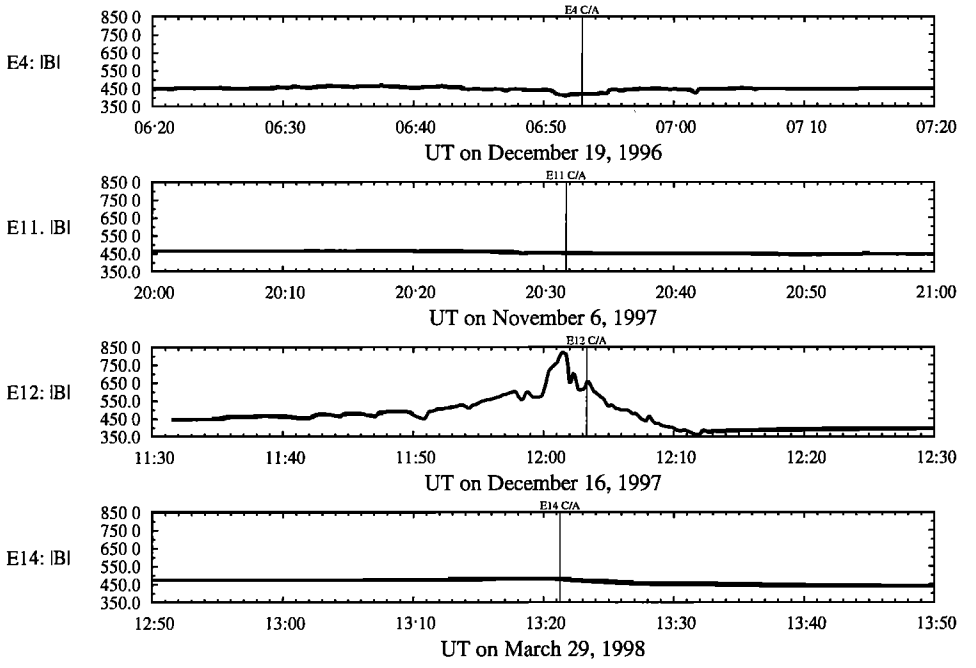

Figure 6. |**B**| in nanotesla versus R (range from Europa in R_E) for four Europa passes plotted with identical scales.

of internal dipolar fields. In order to identify the internal sources of magnetic perturbations, we focus initially on the passes in which signatures of at least a few tens of nanotesla are observed to be on the scale of the moon's radius and localized near the moon. The passes E4 and C9 are most straightforward. In both cases, the trajectory remained very close to the moon's rotational equator. Because the induced dipole moment always lies in the rotational equator, this type of trajectory is especially suited to identifying the signature of an induced field. In both cases, the B_x and B_y components predicted by the induced field model correspond quite closely to the measured values. As noted in section 4, the small amplitudes of the perturbations produced by an induced field signature for both the E11 pass and the E12 pass diminish the value of these passes for interpreting internal sources. For pass E14 the induced field model again gives a satisfactory fit to the B_x and B_y components.

Despite the results from passes E4 and E14 suggesting that induced fields can explain the transverse components of the perturbations, the presence of a small intrinsic dipole field for Europa is not ruled out by the data that we have acquired up until this time. The difficulty is that except for pass E12 on which the signature is dominated by plasma pickup, the encounters up until this time have all occurred at times when the time-varying component of Jupiter's field was predominantly oriented radially outward. The ID model and the perpendicular dipole of the FD-E4 model give very similar predictions for passes E4, E11, and E14 as is evident in Table 2. The model dipoles are all oriented within ±20° of the Jupiter facing meridian with equatorial field magnitude ranging from 92 to 106 nT. Because of the uncertainty regarding the contribution of plasma currents, these values must be regarded as being within the uncertainty of the signatures.

Most of the Europa passes scheduled in the remaining years of GEM will occur north of the center of the torus, implying external field configurations similar to those already encountered as can be seen in Figure 1a. (The trajectories of the passes by Europa and Callisto are shown in Figures 7a and 7b.) The expected induced dipole moments are given in Table 2. Only pass E18 occurs in the southern magnetosphere of Jupiter. For this pass, the induced dipole should lie roughly 150° west of the Jupiter facing meridian with an equatorial field magnitude of 50 nT, and this produces a clear distinction between the predictions of the FD-E4 and ID models. Unfortunately, this pass will be at high altitude (2276 km), and only low time resolution data will be acquired. On pass E16 the altitude will be somewhat lower, recorded data will be available, and the imposed field will be at an angle rotated well to the east of the FD-E4 model, so the distinction will be significant. However, this pass will occur relatively near the center of the plasma sheet, and plasma effects are likely to dominate the perturbations. It may, therefore, prove impossible to differentiate between the two models of internal field contributions on this pass.

For Callisto the distinction between a permanent intrinsic field and an induced field is clearer because passes C3 and C9 were both close encounters, and one occurred above the current sheet while the other occurred below the current sheet. The ID model provides a reasonable approximation to the general trend of the transverse field perturbations for both pass C3 and pass C9. The signature is obscured by plasma-related fluctuations on pass C10. An intrinsic dipole field model can be ruled out for Callisto because any model that fits the C3 perturbations cannot fit the C9 perturbations. We conclude that for Callisto the induced field model provides a plausible interpretation of the observations. Additional passes by Callisto in the GEM mission whose trajectories are shown in Figure 7b will provide further tests of the induced field model.

Table 2. Parameters of Model Dipoles

Model	Angle From Jupiter Facing Meridian	Equatorial Field Magnitude nT
	$\mathbf{M}_\perp$ *for the Europa passes*[a]	
FD-E4[b]	20° west	85
E4: ID	17° east	92
E11:ID	13° west	101
E12:ID	68° east	42
E14:ID	~2° east	106
E15:ID	~135° west	~30
E16:ID	65° east	~42
E17:ID	45° east	~60
E18:ID	150° west	~50
E19:ID	30° west	~60
	$\mathbf{M}_\perp$ *for the Callisto passes*	
FD-C3[c]	0°	14
C3:ID	4° west	16
C9:ID	172° west	17
C10:ID	172° west	15
C20:ID	8° west	17
C21:ID	177° east	10
C22:ID	171° east	21
C23:ID	~8° west	10

[a]Parameters for E4-E14 and C3-C10 from fits. Remaining entries are predicted from the KK97 model.

[b]The projection of a dipole with polar angle 135° relative to Europa's spin axis.

[c]The projection of a dipole with polar angle 80° relative to Callisto's spin axis.

8. Discussion

The signatures from most of the passes by Europa and Callisto show that plasma perturbations are extremely important, particularly near Europa where the indirect signatures of ion pickup are evident. Nonetheless, the systematic variations of the components of the field transverse to the spin axis compellingly support the idea that internal sources also contribute to the perturbations. For Europa it is possible that the internal sources arise either from permanent magnetization or from dynamo action. The evidence that Europa is differentiated and probably has an iron core [*Anderson et al.*, 1997] allows one to take the latter possibility seriously. Nevertheless, at this stage in the data acquisition the possibility that inductive currents flowing within but near the surface contribute the perturbations provides a convincing alternative interpretation. For Callisto the induced field mechanism provides an excellent fit in two cases where the perturbations are significant relative to the background field. Any permanent intrinsic field would be negligibly small. The plasma magnetic fields are expected to be mainly nondipolar and small because Europa and Callisto were outside of Jupiter's plasma sheet when the induction effects were observed.

A conducting shell near the surface can produce perturbations consistent with the observations only if its height-integrated conductivity is sufficiently large. Let us consider the requirements. Suppose that Europa (or Callisto) possesses a conducting shell close enough to the physical surface to be approximated as coincident with that surface. Within this layer, the magnetic field satisfies the equation

$$\nabla^2\mathbf{B} = k^2\mathbf{B} \tag{1}$$

where $k^2 \equiv i\omega\mu\sigma$, σ is the electrical conductivity, ω is the angular frequency of the inducing field $= \Omega_J - \Omega_{\text{moon}}$, i.e., the difference between the angular frequency of Jupiter's rotation, Ω_J, and of the moon's orbital motion, Ω_{moon}, and μ is the permeability (≈ permeability of free space). The inverse magnitude of k is related to δ, the skin depth

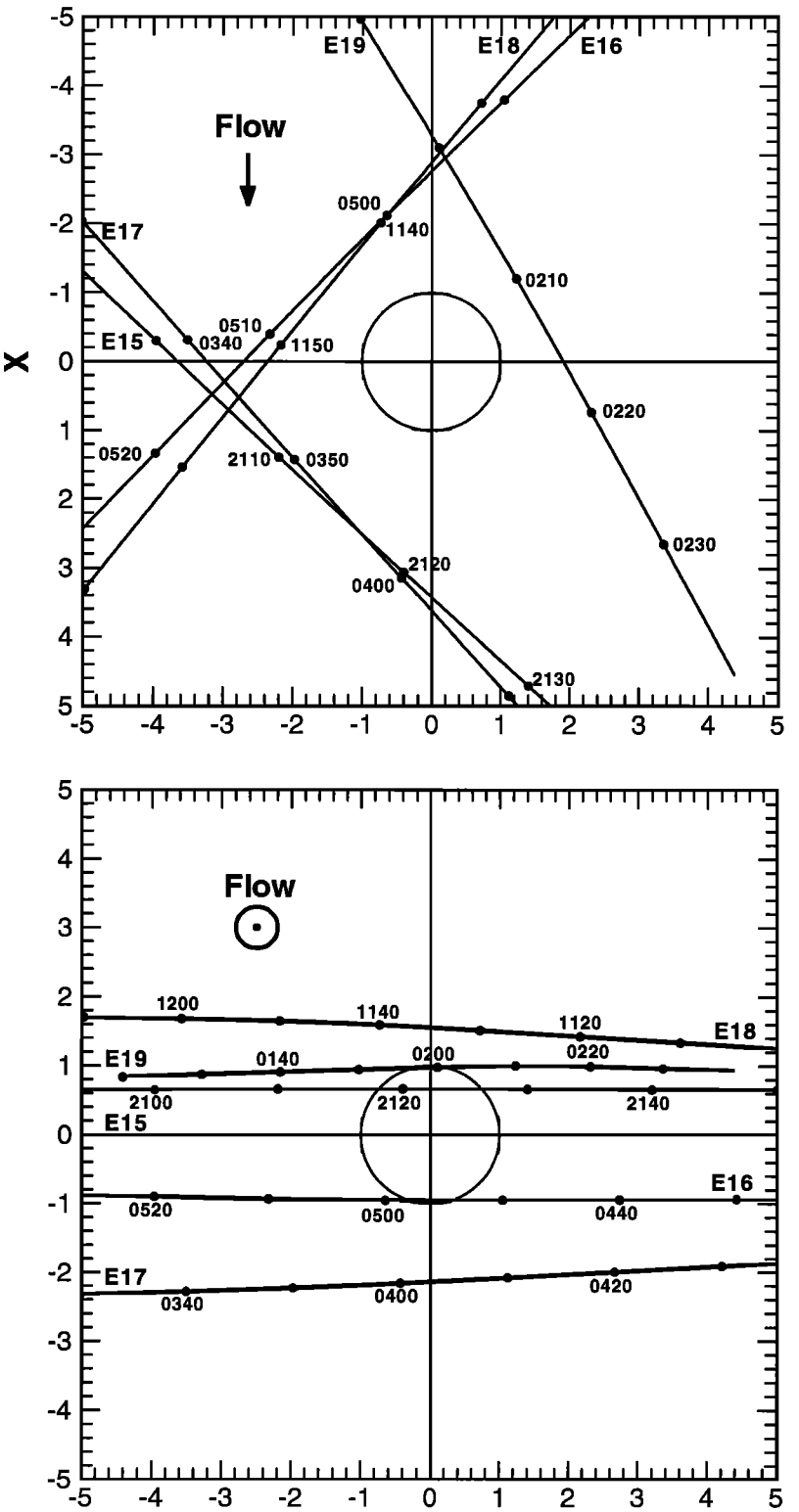

Figure 7a. Same as Figures 3 and 5 but for additional passes by (a) Europa (E15-E19) in the Galileo Europa Mission (GEM) period.

$$\delta = (\sigma\mu\omega/2)^{-1/2} \quad (2)$$

encountered in the analysis of electromagnetic waves in conducting materials. It characterizes the depth to which wave power can penetrate into a conductor.

Both above and below the conducting shell one can approximate the conductivity as that of free space. C. Zimmer et al. (manuscript in preparation, 1998) show that provided $r_s/\delta >> 1$, the response of a very good conductor is approximated for all conductivities and shell thicknesses that satisfy the inequality

$$r_s d/\delta^2 > 5 \quad (3)$$

where d is the shell thickness.

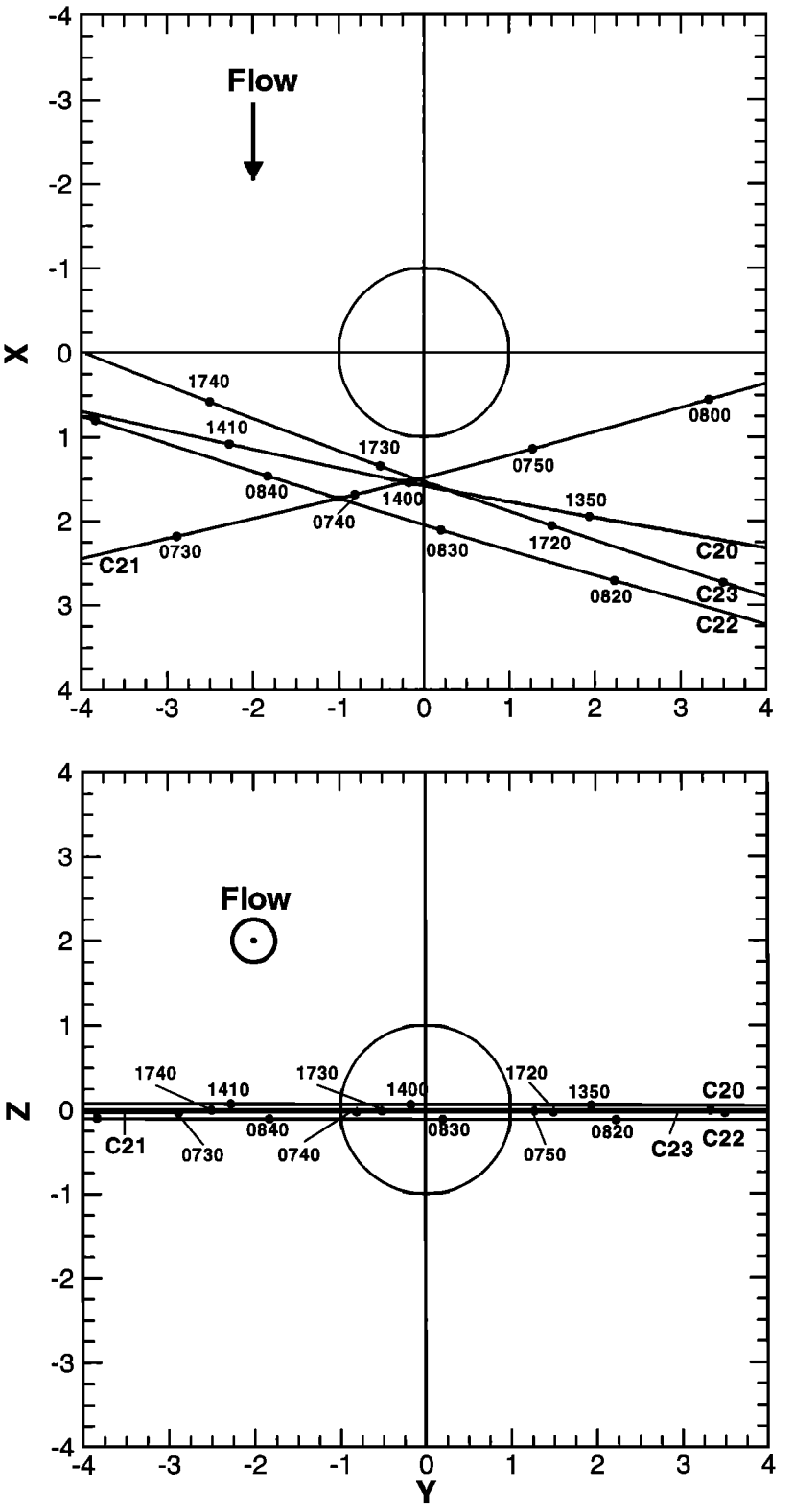

Figure 7b. Same as 7a for Callisto (C20-C23).

One needs to consider the location of the shell where the induced near-surface currents flow. One appealing possibility is that the currents flow in the moon's ionosphere. The existence of an ionosphere at Europa has been reported by *Kliore et al.* [1997] from analysis of radio occultation measurements. Mechanisms for producing the ionosphere have been described by several authors, most recently by *Ip et al.* [1998] and *Saur et al.* [1998]. The proposal that the ionosphere carries the induced currents can be readily rejected. The skin depth determines the minimum thickness of a shell capable of carrying currents large enough to balance the radial component of the time-varying field at its outer boundary. A peak ionospheric conductivity can be estimated from $\sigma_i = n_e e^2/m\omega_{ce}$, where n_e is the electron density, m is the mass of the ionospheric ions, $\omega_{ce} = qB/m_e$ is the electron

gyrofrequency, q is the electron charge, and m_e is the electron mass. In Europa's ionosphere, B = 400 nT and n_e < 10,000 electrons/cm^3 with a scale height of order 240 km [*Kliore et al.*, 1997]. This implies that $\sigma_i < 4 \times 10^{-3}$ S/m. The corresponding skin depth is ~1500 km. Equation (3) then implies that the ionospheric depth would have to be comparable to the lunar radius to carry the required current. Such a deep ionosphere is inconsistent with the limitations imposed by the measured scale height, so an ionospheric closure path must be rejected as the principal cause of the observed signature.

Alternative current closure paths lie within the solid surface of the moons. The possibility that the time-varying component of the Jovian magnetic field might induce currents within the solid body of Europa seems to have been discussed first by *Colburn and Reynolds* [1985]. More recently, others have speculated on this possibility [*Kargel and Consolmagno*, 1996; *Neubauer*, 1998a].

As the surface layers of both Europa and Callisto are icy, a conducting subsurface ocean becomes a possibility. The ocean depth required by equation (3) can be estimated by scaling the shell thickness to 100 km and the conductivity to that of Earth's oceans, ~2.5 S/m at 0°C [*Montgomery*, 1963]. Then we get the requirement on the height-integrated conductivity σd,

$$(\sigma/2.5 \text{ S/m})\,(d/100 \text{ km}) > 0.1 \qquad (4)$$

which means that the ocean can be as salty as Earth's oceans with a thickness of order 10 km, or less salty than Earth's oceans and thicker than 10 km, or some combination of these ranges and still be in the desired regime. Water ice has a conductivity many orders of magnitude too small to work. Dirty ice near its melting point can support induction currents. Unless the outermost part of the rocky core is extensively pervaded by partial melt (water alone is unlikely to do it), it will lack the conductivity to provide the necessary response. Even partial melt may be insufficient. Frozen brine, presumably in veins or cracks, might provide conductivity paths through an otherwise pure ice layer, but this conductivity would still be less than that of salty water by an order of magnitude or more and would moreover apply only to a small fraction of the surface area of the satellite. Ice near melting point or capillary channels within a porous layer are conceivable, but it may be difficult to develop thermal models that remain near melting over tens of kilometers with no melted layer.

In applying the induced field model to Europa and Callisto, we have assumed high conductivity with the current-carrying layer very close to the surface. If the conducting layer were below the surface at a radial distance r_d from the center, the signal would decrease in amplitude with distance r from the center as $(r_d/r)^3$ and it would be smaller than the observations by a factor of about $(r_d/r_s)^3$ where r_s is the radius of the moon. Thus an ocean whose upper boundary is 10 km below the surface of Europa would account for the data. On the other hand, if the ocean were buried 100 km beneath the surface, the induced field would be smaller than we have calculated by a factor of ~0.8, and it would not fit the data well. At Callisto, burying the ocean 100 km below the satellite surface would decrease the predicted field by 0.88, resulting in a significant but possibly acceptable mismatch to the data.

Although others have considered the existence of a subsurface ocean on Europa, models of the interior have not taken the possibility of oceans within Callisto seriously. Callisto's surface appears geologically dead, with features that appear to have persisted since early times except for processes related to impacts and surface sublimation. Although it is partly differentiated, Callisto's gravitational field indicates that it is by far the least differentiated of the Galilean satellites [*Anderson et al.*, 1998]. Images show an unexpected degree of sublimation-driven processes that might conceivably indicate a warm interior closer to the surface than that generally supposed. On the basis of an examination of the previously published dipole moment obtained from the C3 data [*Khurana et al.*, 1997], *Neubauer* [1998a] suggested the possibility of induced currents within Callisto presumably flowing in an ocean. The additional data from pass C9 and the success of the induced field model in fitting data from both passes leads us to support his suggestion.

Thus our data support compellingly the unexpected result that Callisto has a salty water ocean or perhaps some other melted or partly melted layer more than 10 km thick (see equation (4)) that can conduct electricity and that is located only a small fraction of the satellite radius beneath the surface. The latter is a surprising result, even in light of the new data on the moment of inertia that imply a partially differentiated structure [*Anderson et al.*, 1998]. Certainly, there is no problem in placing an ocean near the minimal melting point of water ice, which occurs at 200 km depth (a pressure of 2 kbar), but the magnetic field suggests an ocean that is closer to the surface.

For Europa the distinction between an induced field and a permanent dipole moment whose component perpendicular to the spin axis has a surface equatorial field of order 100 nT is not secure on the basis of the data available at this time. There are two compelling arguments that the source of the transverse dipole moment is inductive. First, it seems improbable that a model with no adjustable parameter works as well as it does if it has no basis in reality. Second, the large tilt required by the FD-E4 model (45° from the spin axis), while not impossible, would differ markedly from the small tilts observed for other solid magnetized bodies. (Neptune and Uranus differ by having relatively poorly electrically conducting dynamos in "icy" interiors [*Connerney*, 1993].) Thus, for Europa as well as Callisto, we favor the induced field model as the explanation of the observed $\mathbf{M}_\perp$. For Europa an additional contribution from a permanent $\mathbf{M}_z$ with a surface equatorial field of order 100 nT cannot be excluded on the basis of the present analysis. Corrections to both models for the effects of Alfvén wing currents [*Neubauer*, 1998b] will also be needed to more accurately represent the observations. Fortunately, the predictions of the two competing models on at least one of the orbits in the GEM mission may differ enough to provide a critical test provided that the background field remains relatively undisturbed.

9. Conclusion

We have argued that the magnetic perturbations observed in the Galileo passes near Europa and Callisto can be interpreted as the signatures of induced dipole moments arising from currents flowing in near-surface conducting shells. For each pass, the strength and orientation of the induced magnetic moment are governed by the instantaneous local value of the time-varying component of Jupiter's magnetic field. The interpretation is not unambiguously supported by the data from the four Europa passes that we have analyzed. However, this model (which, as we noted in section 8, makes explicit predictions with no free parameters) gives a reasonable lowest-order fit to the observations in the cases for which the expected signature of the induced field is larger than signatures that we associate with plasma currents. Departures from the predictions of the model can in all cases plausibly be attributed to the ambient plasma. Thus we believe that the induced field model and the implication that a subsurface conducting layer exists on both moons deserve serious consideration.

The observed magnetic field perturbations require a comet-like interaction between Europa and Jupiter's plasma sheet. The intensity of the interaction is modulated by System III longitude. Related phenomena such as the structure of Europa's ionosphere and the strength of the current system coupling Europa to Jupiter's ionosphere are expected to reveal analogous systematic changes if ordered by Europa's System III longitude.

Acknowledgments. We are grateful to Duane Bindschadler of the Jet Propulsion Laboratory for support in all phases of data collection and to Joe Mafi for data processing and preparation of data plots. The work reported here was partially supported by the Jet Propulsion Laboratory under contract JPL 958694.

Janet G. Luhmann thanks Jeffrey S. Kargel and Fritz M. Neubauer for their assistance in evaluating this paper.

References

Anderson, J. D., E. L. Lau, W. L. Sjogren, G. Schubert, and W. B. Moore, Europa's differentiated internal structure: Inferences from two Galileo encounters, *Science, 276*, 1236, 1997.

Anderson, J. D., G. Schubert, R. A. Jacobson, E. L. Lau, W. B. Moore, and W. L. Sjogren, Distribution of rock, metals, and ices in Callisto, *Science, 280*, 1573, 1998.

Bagenal, F., Empirical model of the Io plasma torus: Voyager measurements, *J. Geophys. Res., 99*, 11043, 1994.

Cheng, A.F., P. K. Haff, R. E. Johnson, and L. J. Lanzerotti, Interactions of planetary magnetospheres with the icy satellite surfaces, in *Satellites*, edited by J.A. Burns and M.S. Mathews, 403, Univ. of Ariz. Press, Tucson, 1986.

Colburn, D.S., and R. T. Reynolds, Electrolytic currents in Europa, *Icarus, 63*, 39, 1985.

Connerney, J. E. P., Magnetic fields of the outer planets, *J. Geophys. Res., 98*, 18659, 1993.

Dessler, A. J., Coordinate systems, in *Physics of the Jovian Magnetosphere*, edited by A. J. Dessler, p. 498, Cambridge Univ. Press, New York, 1983.

Eviatar, A., G. L. Siscoe, T. V. Johnson, and D. L. Matson, Effects of Io ejecta on Europa, *Icarus, 47*, 75, 1981.

Eviatar, A., A. Bar-Nun, and M. Podolak, Europan surface phenomena, *Icarus, 61*, 185, 1985.

Goertz, C.K., Io's interaction with the plasma torus, *J. Geophys. Res., 85*, 2949, 1980.

Gurnett, D.A., W. S. Kurth, R. R. Shaw, A. Roux, R. Gendrin, C. F. Kennel, F. L. Scarf, and S. D. Shawhan, The Galileo plasma wave system, *Space Sci. Rev., 60*, 341, 1992.

Gurnett, D.A., W. W. Kurth, A. Roux, S. J. Bolton, E. A. Thomsen, and J. B. Groene, Galileo plasma wave observations near Europa, *Geophy. Res. Lett., 25*, 237, 1998.

Intriligator, D. S., and W. D. Miller, First evidence for a Europa plasma torus, *J. Geophys. Res., 87*, 8081, 1982.

Ip, W.-H., Europa's oxygen exosphere and its magnetospheric interaction, *Icarus, 120*, 317, 1996.

Ip, W.-H., D. J. Williams, R. W. McEntire, and B. H. Mauk, Ion sputtering and surface erosion at Europa, *Geophys. Res. Lett., 25*, 829, 1998.

Kargel, J. S., and G. J. Consolmagno, Magnetic fields and the detectability of brine oceans in Jupiter's icy satellites, *Lunar Planet. Sci., XXVII*, 643, 1996.

Khurana, K.K., Euler potential models of Jupiter's magnetospheric field, *J. Geophys. Res., 102*, 11295, 1997.

Khurana, K.K., M.G. Kivelson, C.T. Russell, R.J. Walker, and D.J. Southwood, Absence of an internal magnetic field at Callisto, *Nature, 387*, 262, 1997.

Khurana, K.K., M.G. Kivelson, D.J. Stevenson, G. Schubert, C.T. Russell, R.J. Walker, S. Joy, and C. Polanskey, Induced magnetic fields as evidence for subsurface oceans in Europa and Callisto, *Nature, 395*, 749, 1998.

Kivelson, M.G., K.K. Khurana, J.D. Means, C.T. Russell, and R.C. Snare, The Galileo magnetic field investigation, *Space Sci., Rev., 60*, 357, 1992.

Kivelson, M.G., K.K. Khurana, S. Joy, C.T. Russell, R.J. Walker, and C. Polanskey, Europa's magnetic signature: Report from Galileo's first pass on December 19, 1996, *Science, 276*, 1239, 1997.

Kliore, A. J., D. P. Hinson, F. M. Flasar, A. F. Nagy, and T. E. Cravens, The ionosphere of Europa from Galileo radio occultations, *Science, 277*, 355, 1997.

Linker, J.A., M.G. Kivelson, and R.J. Walker, A three-dimensional MHD simulation of plasma flow past Io, *J. Geophys. Res., 96*, 21037, 1991.

Montgomery, R. B., Oceanographic data, in *American Institute of Physics Handbook*, pp. 125-127, McGraw-Hill, New York, 1963.

Neubauer, F. M., Nonlinear standing Alfvén wave current system at Io: Theory, *J. Geophys. Res., 85*, 1171, 1980.

Neubauer, F. M., The sub-Alfvénic interaction of the Galilean satellites with the Jovian magnetosphere, *J. Geophys. Res., 103*, 19843, 1998a.

Neubauer, F. M., Modification of the Alfvén wing model by electromagnetic induction in the interior of the Galilean satellites, in *Abstracts: The Jovian System After Galileo, The Saturnian System Before Cassini-Huygens*, mtg. abstract, Nantes, France, p. 93, 1998b.

Paterson, W.R., L.A. Frank, and K.L. Ackerson, Galileo observations of pickup ions at Europa, *Eos Trans. AGU, 79*(17), Spring Meet. Suppl. S201, 1998.

Saur, J., D. F. Strobel, and F. M. Neubauer, Interaction of the Jovian magnetosphere with Europa: Constraints on the neutral atmosphere, *J. Geophys. Res., 103*, 19947, 1998.

Schreier, R., A. Eviatar, V. M. Vasyliunas, and J. D. Richardson, Modeling the Europa plasma torus, *J. Geophys. Res., 98*, 21231, 1993.

Southwood, D.J., M. G. Kivelson, R. J. Walker, and J. A. Slavin, Io and its plasma environment, *J. Geophys. Res., 85*, 5959, 1980.

L. Bennett, S. Joy, K.K. Khurana, M.G. Kivelson, C.T. Russell, R.J. Walker, and C. Zimmer, University of California, Institute of Geophysics and Planetary Physics, 6843 Slichter Hall, 405 Hilgard Avenue, Los Angeles, CA 90095-1567. (e-mail mkivelson@igpp.ucla.edu)

C. Polanskey, Jet Propulsion Laboratory, 4800 Oak Grove Drive, Pasadena, CA 91109.

D.J. Stevenson, Division of Geological and Planetary Sciences, California Institute of Technology, Pasadena, CA 91109.

(Received May 26, 1998; revised October 29, 1998;
accepted November 2, 1998.)